Kazano et al. Mechanics of Advanced Materials and Modern Processes (2018) 4:6
https://doi.org/10.1186/s40759-018-0039-3

Mechanics of Advanced Materials and Modern Processes

RESEARCH Open Access

Experimental and analytical investigation on resin impregnation behavior in continuous carbon fiber reinforced thermoplastic polyimide composites

Shota Kazano[1], Toshiko Osada[1], Satoshi Kobayashi[1*] and Ken Goto[2]

Abstract

In molding of carbon fiber reinforced thermoplastics (CFRTP), resin impregnation behavior to fiber yarns is very important because higher viscosity of molten thermoplastics inhibites resin impregnation to the interspace among fibers. Resultant resin un-impregnation causes lower mechanical properties of CFRTP. The purpose of this study was to clarify the relation among molding method, molding conditions and resin impregnation to fiber yarns experimentally and analytically. In this study, CFRTPs using continuous carbon fiber yarn as a reinforcement and a thermoplastic polyimide which is excellent in heat resistance as a matrix resin were produced by Micro-Braiding, Film Stacking and Powder method. In addition resin impregnation was modeled based on Darcy's law and continuity condition. As a result, analytical resin impregnation prediction showed good agreements with the experimental results in all the producing methods and molding conditions. In addition, the void content in the molded CFRP could be greatly reduced by pressurizing cooling.

Keywords: CFRTP, Resin impregnation, Micro-braiding, Darcy's law

Introduction

Since carbon fiber reinforced plastics (CFRP) has excellent characteristics of specific strength and specific stiffness, it has been used in many fields including aerospace. The thermosetting resins generally used for CFRP are relatively brittle compared with thermoplastic resins, and is also inferior in impact resistance (Lee and Kim 2017). Furthermore, CFRP is generally molded by heat-pressurizing using a semi-cured prepreg sheet impregnated with thermosetting resin to carbon fibers, so that it takes time for polymerization reaction (Svensson et al. 1998). In addition, the prepregs need to be stored at low temperature, resulting in high cost for equipment.

On the other hand, thermoplastic resins have excellent toughness and impact resistance, and are easy to handle as compared with thermosetting resins. In addition, because carbon fiber reinforced thermoplastics (CFRTP) can be remolten, it has good formability and recyclability. There is also an advantage that it can be stored at room temperature. Moreover CFRTPs using super engineering plastics are expected to have excellent heat resistance and mechanical properties (Rattanand Bijwa 2006, Bijwa and Rattan 2007).

Thermoplastics and their composite have superior properties as mentioned above, however, they have inferior characteristics such as lower resin impregnation to reinforcing fiber yarns. The reason is higher melt viscosity of thermoplastic resin. Thus resin-un-impregnated region, referred as void, exists in the fiber yarns after molding, which fact results in lower mechanical properties.

Therefore, various molding methods to achieve sufficient thermoplastic resin impregnation to fabrics consisted of continuous fiber yarns have been studied for the practical usage of the composites in structural members.

Examples for CFRTP molding include Film Stacking (FS) method (John et al. 1999b; Fujihara and Harada

* Correspondence: koba@tmu.ac.jp
[1]Department of Mechanical Engineering, Graduate School of Science and Engineering, Tokyo Metropolitan University, 1-1 Minami-Osawa, Hachioji, Tokyo 192-0397, Japan
Full list of author information is available at the end of the article

2000; Thomas et al. 2013), Powder method (Lin et al. 1994; Lin and Friedrich 1995), Co-Woven method (Clemans et al., 1987), Commingled Yarn (CY) method (Lin et al. 1995) and Micro Braiding (MB) method (Sakaguchi et al. 2000; Fujihara et al. 2003; Kamaya et al. 2001; Hung 2004). Film Stacking (FS) method (John et al., 1999; Fujihara and Harada 2000; Thomas et al. 2013) is the method to hot-compression molding with alternately laminated woven fabrics and film-like polymer sheets. Powder method (Lin et al. 1994, Lin and Friedrich 1995) uses fiber yarns attached with pulverizing thermoplastic resin. Co-Woven method (Clemans et al. 1987) is a method of alternately weaving resin fiber yarns and reinforcing fiber yarns into one fabric. Commingled Yarn (CY) method (Lin et al. 1995) uses commingled yarn with fiberized thermoplastic resin and reinforcing fiber. In Micro-Braiding (MB) method (Sakaguchi et al. 2000; Fujihara et al. 2003; Kamaya et al. 2001; Hung 2004), a braided fibrous intermediate material (Micro-Braided Yarn) composed of reinforcing fiber yarns at the center and thermoplastics fibers around them are prepared with traditional braiding technique. The resin fibers are assembled around the reinforcing fibers and are evenly adhered. Thus improvement in impregnation property is expected.

Many experimental researches have been conducted to improve the impregnation property of the thermoplastic resin to the reinforcing fiber yarns. In addition, analytical approaches about resin impregnation to fiber yarns have been conducted. As for the impregnation behavior of thermoplastic resin, Wolfrath et al. (2006) analyzed the impregnation of the polypropylene to the fiber yarns in the FS method based on the Darcy's law and discussed the impregnated state of each layer as a function of time and pressure. Bernet et al. (1999) conducted a resin impregnation analysis for the CY method to evaluated the quality of the molded article with the void content. Lin et al. (1994) also evaluates the impregnation behavior for the Powder method based on the Darcy's law analytically. Furthermore, West et al. (1991) assumed the fiber yarn to be elliptical and defined the equivalent impregnation radius corresponding to the impregnation distance of the circular model.

As described above, the Darcy's law has been used for resin impregnation analysis to fiber yarns. The Darcy's law represents apparent flow velocity with pressure gradient, viscosity of fluid and permeability. The permeability is considered to depend on the geometry of the fibers composing the fiber yarn. (Gutowski 1985, Gutowski et al, 1987) evaluated the permeability coefficient depending on the fiber volume fraction based on the fiber yarn compression model. Furthermore, permeability coefficient was also predicted with a geometric model. Gebart (1992) classifies the orientation state of circular cross section of fiber into a square array or a hexagonal array, and permeability of fiber yarn perpendicular direction was derived from Navier-Stokes equations. For thermoplastic resin, Kim et al. (1989) evaluates the permeability of PEEK for unidirectional fiber yarn with Carnam-kozeny constant using similar analytical method to Gutowski et al. (1985). Also, in the same analytical method, Hou et al. (1998) predicts the void content of molded parts of CF/PEI composites.

As described above, many researches on resin impregnation behavior in FS, CY and Powder method could be confirmed. On the other hand, there are some researches about MB method (Sakaguchi et al. 2000; Fujihara et al. 2003; Kamaya et al. 2001; Hung 2004; Kobayashi et al. 2012a, b; Kobayashi and Tanaka 2012; Kobayashi and Takada 2013) for unidirectional composites, whereas the resin impregnation behavior for continuous woven materials has been limited (Kobayashi and Morimoto 2014; Kobayashi et al. 2014, 2017) because of their complexity. However, it is important to clarify the resin impregnation behavior for continuous woven material with superior in drape property compared to unidirectional material, considering actual usage of the composites (Kobayashi et al. 2017). In the analysis of impregnation behavior in continuous fiber yarns, it has been reported that by assuming that all the fiber yarns are simultaneously impregnated in the laminate and they are all identical in geometry can be described by impregnation with only a typical single yarn (Lin et al. 1995). The cross-section of such a fiber yarn is roughly elliptical after initial compression. Since it can be assumed that this cross section exists along the entire length of the fiber yarn, it is considered that a two-dimensional analysis of resin impregnation to fiber yarn is appropriate.

In this research, we investigated the effect of molding method and molding conditions on resin impregnation to fiber yarns in CFRTP. Carbon woven fabric and thermoplastic polyimide (PI), which is a super engineering plastics with superior heat resistance, were used. CFRTPs were prepared with MB, FS and Powder methods, and the resin impregnation properties were evaluated experimentally. Furthermore, we focused on the two-dimensional resin impregnation analysis and analytical resin impregnation prediction was conducted based on the previous research (Kobayashi et al. 2017) to discuss the difference in impregnation behavior in different molding methods.

Experiment method

Materials

In this study, carbon fiber yarns, T300B-3000 filaments (3 K) or T700SC-12,000 (12 K) filaments (Toray) were used as the reinforcements to evaluate yarn thickness on resin impregnation, and a thermoplastic polyimide (PI, AURUM PL 450 C, Mitsui Chemicals) was used as the base material resin. Table 1 shows properties of PI. In FS

Table 1 Properties of PI matrix (from Mitsui Chemical)

AURUM-PL450C	
Viscosity [Pa s]	600 (at 410 °C)
Melting Point [°C]	390
Density [g/cm^3]	1.33
Tex for PI yarn [g/1000 m]	60

and Powder methods, pre-woven fabric (CO6343B or CK6261C, Toray) consisted of T300B or T700SC described above were used. In MB methods, MBYs were fabricated with PI fiber yarns on a medium-class braider and plain woven fabrics were weaved with MBY on a hand looms. The fabrics were cut into sheets of square, 75 mm, which include 40 yarns for 3 K and 21 yarns for 12 K.

PI films with thickness 50 μm were used in FS methods. For PI methods, PI powder was prepared with PI pellets using a pulverizer (SM-1, HISIANGTAI). PI resin powder with diameter 50 to 200 μm obtained with a test sieve (mesh opening 425 μm) was used. In the manufacturing process of MBY, a reinforcing fiber yarn was located at the center of the braider and matrix resin fiber yarns were braided around the reinforcing fiber yarn. In the present study, fiber volume fraction was 38.4% in all methods.

CFRTP fabric textile molding

CFRTP textile composites were compression-molded with a hot press system (IMC-1837, Imoto Machinery). Molding conditions are shown in Table 2. We selected the pressure values to obtain full impregnation in molding time less than 5 min considering practical process time. Fabrics and matrix resin, or fabrics made of MBY were placed in a mold at room temperature, and the mold was placed on the lower platen of a hot press machine preheated to 350 °C and heated to a molding temperature. When mold temperature reached the test temperature, pressure was applied to the mold. The time at the beginning of pressurizing was defined as molding time 0 s. After the pressure was maintained during the molding time, the pressure was relieved and the mold was air-cooled until 50 °C.

The PI resin used in this study has high heat resistance and high melting point, and the molding temperature

Table 2 Molding condition

Molding Method	Molding Temperature [°C]	Volume Fraction of Fiber [%]	Number of Filament	Number of Lamination	Molding Pressure [MPa]	Molding Time [s]	A Piece of Textile [mm]	Pressure Cooling (PC)
Micro-Braiding			3 K	4	2	300	75	○
						0, 20, 30, 60, 120, 180, 240, 300		–
					4	0, 60, 120, 180, 240, 300		–
Film Stacking	410	38.4	3 K	1	0, 1, 2,4, 8	900	75	–
				4	0	0, 300		–
					2	300		○
						0, 20, 30, 60, 120, 180, 240, 300		–
					4	0, 60, 120, 180, 240, 300		–
			12 K		0	0		–
					4	0, 300		–
					8	300		–
Powder			3 K	1	0, 0.1, 0.3, 0.5, 0, 1, 2, 4	900	150	–
				4	0.3, 0.5, 1, 2, 4			–
					0	0, 300	75	–
					2	300		○
						0, 20, 30, 60, 120, 180, 240, 300		–
					4	0, 60, 120, 180, 240, 300		–
			12 K		0	0		–
					4	0, 300		–
					8	300		–

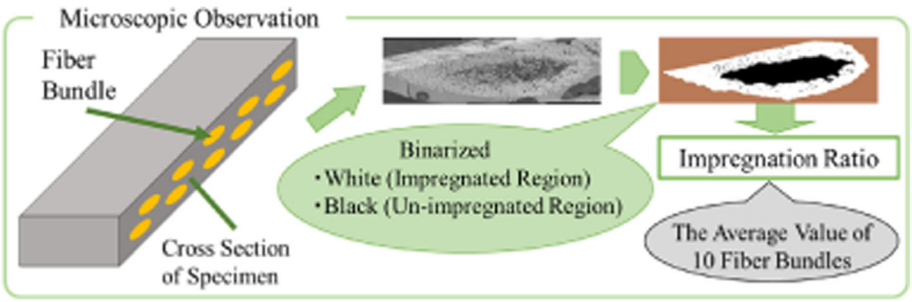

Fig. 1 The schematic view of the resin impregnation ratio measurement

was determined as 410 °C (viscosity; 600 Pa·s) from a supplier data. Since the hot press system used could heat up to 350 °C which is lower than the molding temperature, the mold was implemented with additional four cartridge heaters (200 V -1400 W) which result in higher molding temperature. The mold temperature and the pressure loaded on the specimen were defined as molding temperature and molding pressure. In this study, in order to investigate void dissipation behavior, non-pressurizing cooling (NPC) and pressurizing cooling (PC) were conducted during cooling in the molding process.

Cross-sectional observation

In order to measure impregnation ratio as a function of molding conditions, cross sectional observation was performed at the center of the specimen molded under each condition. After the molded specimen was embedded in epoxy resin, the cross-section was polished using # 180–2000 emery papers, and the section was buffed with alumina slurry (0.3 μm, Maruto Co.). The polished surface was observed using a digital-microscope (VH-Z100R, KEYENCE) having a zoom lens which enables to confirm a cross-section of a single carbon fiber. The digital image obtained was converted into a binary bitmap image using software (GIMP 2). The resin impregnation ratio was calculated as the ratio of the number of pixels in the impregnated region including the cross-sectional area of the fiber yarn to that of pixels in the whole cross section of the yarn. Since a moderate scatter was observed, the average value was shown as the result. The schematic view of the resin impregnation ratio measurement is shown in Fig. 1.

Analysis

Calculation of impregnation ratio of elliptical model (Kobayashi et al. 2017)

In order to fully demonstrate the mechanical properties of reinforcing carbon fibers in CFRTP, complete impregnation of the resin to reinforcing fiber yarns is necessary. Thus it is an important to analytically-predict the time necessary for complete resin impregnation to yarns. In the present study, resin impregnation behavior was analytically predicted similar to the previous study (Kobayashi et al. 2017).

The fiber yarn is considered as a porous medium, where the gap between fibers is regarded as pore. In general, the impregnation phenomenon of the rein to fiber yarns is regarded as laminar flow to a porous medium and represented using the Darcy's law (Åström et al. 1992). The Darcy's law is expressed as,

$$u = -\frac{k}{\mu} \cdot \frac{\partial P}{\partial x} \tag{1}$$

where u is Darcy's velocity, μ is the viscosity, $\partial P / \partial x$ is the pressure gradient, and k is the permeability coefficient.

Also, an equation of continuity can be written as,

$$\nabla \cdot \mathbf{u} = 0 \tag{2}$$

In the present study, the cross-section of a fiber yarn was deformed to an elliptical shape by compression loading. Thus it is assumed that the fiber yarn has a cross section close to an elliptical shape with major radius a_0 (x direction) and minor radius b_0 (y direction),

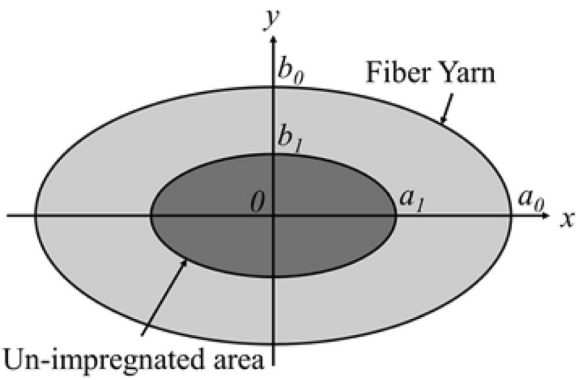

Fig. 2 Coordinate of elliptical fiber yarn model

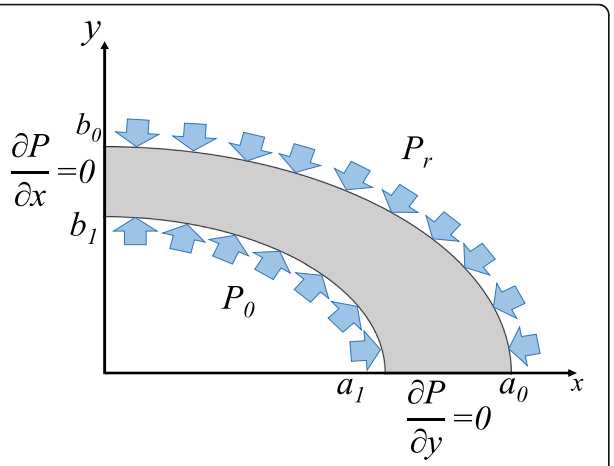

Fig. 3 Boundary condition of quarter elliptical fiber yarn model

as shown in Fig. 2. The fiber longitudinal direction is defined as z.

As shown in Fig. 2, an oval un-impregnated region where major and minor radii are a_1 and b_1 respectively, is assumed. a_1 and b_1 become shorter with molding time and resultant resin impregnation.

By using the fiber volume fraction V_f in the fiber yarn and the eq. (1), Darcy's velocity is converted to flow front velocity in x direction.

$$(1-V_f)\frac{da_1}{dt} = u_x|_{x=a_1} = -\frac{k}{\mu}\cdot\frac{\partial P}{\partial x}\bigg|_{x=a_1} \tag{3}$$

By re-arranging and integrating both sides,

$$a_1 = -\frac{k}{\mu(1-V_f)}\int\frac{\partial P}{\partial x}dt \tag{4}$$

In the same way, the following equation is obtained for the y direction.

$$b_1 = -\frac{k}{\mu(1-V_f)}\int\frac{\partial P}{\partial y}dt \tag{5}$$

In the elliptical model as shown in Fig. 2, the cross-sectional area of the fiber yarn and the cross-sectional area of the non-impregnated region are $S_0 = \pi a_0 b_0$ and $S_1 = \pi a_1 b_1$, respectively, so that the impregnation ratio I becomes.

$$I(t) = 1-\frac{\pi a_1 b_1}{\pi a_0 b_0} = 1-\frac{a_1(t)b_1(t)}{a_0 b_0} \tag{6}$$

The pressure gradient of the coordinates (a_1, 0) and (0, b_1) at the flow front of the resin shown in Fig. 2 should be obtained to calculate the position of the flow front from eqs. (4) and (5) and resultant impregnation ratio represented by eq. (6) at a certain time t.

Calculation of pressure gradient in elliptical model

In the present study, resin flow in the axial direction is neglected. In orthogonal coordinates as shown in Fig. 2, since the flow velocity u_z in the z direction is assumed as 0, eq. (2) can be expressed as follows.

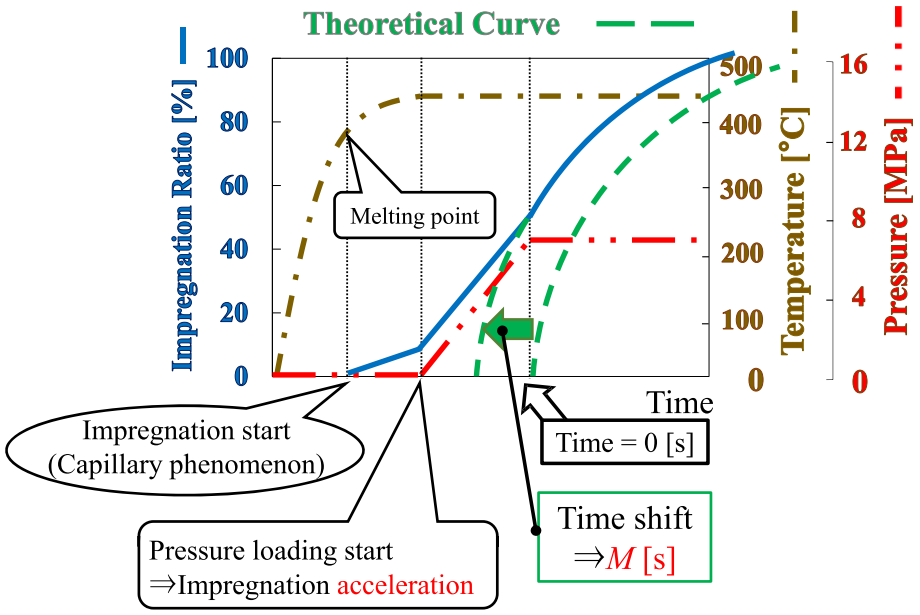

Fig. 4 Modification of analytical impregnation ratio curve

$$\nabla \mathbf{u} = \frac{\partial u_z}{\partial x} + \frac{\partial u_y}{\partial y} = 0 \tag{7}$$

Here, substituting eq. (3) into eq. (7) and assuming that the melt viscosity μ and the permeability coefficient k of the resin are independent of time, the following equation is obtained.

$$\frac{\partial^2 P}{\partial x^2} + \frac{\partial^2 P}{\partial y^2} = 0 \tag{8}$$

In this case, the boundary condition for the elliptical model as shown in Fig. 2 is defined as follows.

1: $P=P_m$ (resin pressure) on the outer boundary of the elliptical fiber yarn ($\frac{x^2}{a_0} + \frac{y^2}{b_0} = 1$).

2: $P=P_0$ (atmospheric pressure) on the boundary of the elliptical un-impregnated region ($\frac{x^2}{a_1} + \frac{y^2}{b_1} = 1$).

Since the elliptical model shown in Fig. 2 is symmetrical to the x and y axes, the pressure distribution for the resin impregnation to the fiber yarn in the 1/4 model as shown in Fig. 3 shall be considered. The pressure gradient at the flow front could be obtained from the pressure distribution. It is, however, difficult to solve eq. (8) analytically, a mathematical approach was carried out by using the boundary element method.

Eqs. (4) and (5) are discretized in terms of time t, when $t = t_i = i\Delta T$ (i: natural number), as

$$a_1(t_i) = a_0 - \sum_{j=1}^{i-1} \frac{k}{\mu(1-V_f)} \frac{\partial P}{\partial x}\bigg|_{x=a_1(t_j)} \cdot \Delta t \tag{9}$$

$$b_1(t_i) = b_0 - \sum_{j=1}^{i-1} \frac{k}{\mu(1-V_f)} \frac{\partial P}{\partial y}\bigg|_{x=b_1(t_j)} \cdot \Delta t \tag{10}$$

where a_0 and b_0 are the positions of flow front at $t = 0$ considering capillary effect.

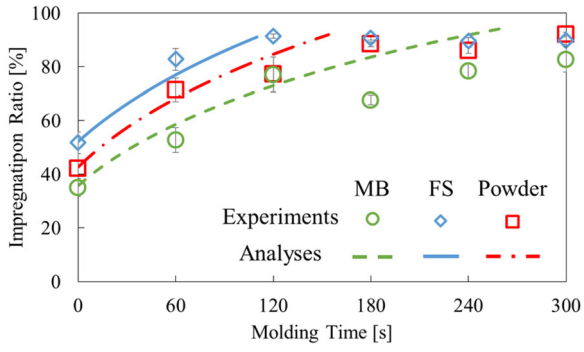

Fig. 5 Effect of molding time on resin impregnation behavior in 3 K composites (Molding pressure: 2 MPa)

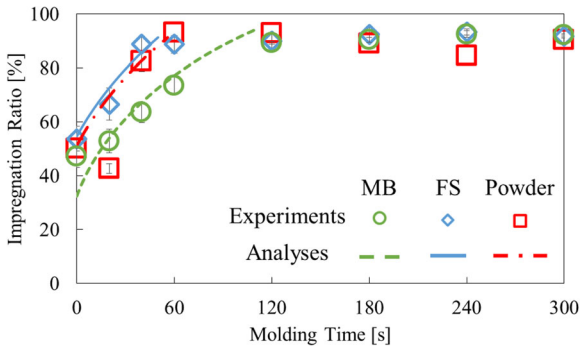

Fig. 6 Effect of molding time on resin impregnation behavior in 3 K composites (Molding pressure: 4 MPa)

Permeability

In the present study, permeability, k, is calculated according to the Kozeny-Carman equation (Gutowski 1985) as,

$$k = \frac{{d_f}^2}{16k_0} \frac{(1-V_f)^3}{{V_f}^2} \tag{11}$$

where d_f is the diameter of a single fiber and k_0 is the Kozeny constant. This equation is known as the permeable Kozeny-Carman equation.

Generally, the fiber volume fraction is related to the applied pressure. Gutowski (1985) derived this relationship in consideration of the elastic deformation of the fiber yarn. Assuming a quasi-static loading, the relationship between pressure and fiber volume fraction is expressed as,

$$P_m - P_0 = A \frac{\sqrt{\frac{V_f}{V_0}} - 1}{\left(\sqrt{\frac{V_a}{V_0}} - 1\right)^4} \tag{12}$$

where P_a is the molding pressure, P_0 is the atmospheric pressure, A is the experimental spring constant, v_a is the maximum possible fiber volume fraction, and v_o is the no-load volume fraction.

Correction of resin infiltration ratio by capillary phenomenon

The impregnation ratio can be obtained with respect to time based on the theory described above. On the other hand, the actual resin impregnation to a fiber yarn occurs before temperature and pressure reach the target

Table 3 Parameters used in the analysis

	MB, FS, Powder	
	2 MPa	4 MPa
k [m^2]	4000×10^{-18}	3073×10^{-18}
k_0 [–]	138	138
M [s]	−34	−34

Table 4 Geometric parameters for carbon fiber yarns

	Method	Major Axis [μm]	Minor Axis [μm]	Aspect Ratio [–]
2 MPa	MB	1607.3	371.1	4.4
	FS	1440.0	184.4	7.8
	Powder	1463.6	201.5	7.3
4 MPa	MB	1437.2	365.7	4.0
	FS	1478.6	179.4	8.2
	Powder	1490.2	184.3	8.1

values because of capillary action. For example, resin impregnation was confirmed at molding time = 0 s as described below. In this study, the influence of capillary action is not analytically considered. In order to consider the capillary action semi-quantitatively, the predicted curve was sifted in the time direction as shown in Fig. 4. Here the time shift is defined as M value. Effect of molding condition on the M values are also discussed later.

Result and discussion

Effect of molding time and molding method (3 K-4 plies–MB. FS, powder)

Figures 5 and 6 show the effect of molding time on the resin impregnation behavior for each molding pressure (2, 4 MPa) and molding method. Due to the increase in molding pressure, the following two affect on the resin impregnation behavior; 1. the promotion of resin impregnation caused by increasing flow rate of molten resin, and 2. the decrease in permeability due to the increase in fiber volume fraction. In the present case, the resin impregnation was promoted with increasing molding pressure, which result suggest that the molding pressure acted as a driving force for resin impregnation.

In order to predict resin impregnation process, impregnation ratio as a function of time at molding pressure 2 and 4 MPa were curve-fitted by choosing the permeability coefficient k and M value defined in section 3.4 as shown in Table 3. We conducted calculation iteratively by selecting k and M values to obtain the parameters to fit the experimental results until correlation coefficient more than 0.92. The geometric parameters for carbon fiber yarn were also shown in Table 4. From the eqs. (11) and (12), the permeability coefficient at an arbitrary molding pressure could be obtained with the Kozeny constant k_0. The parameters included in the equation were assumed as shown

Table 5 Parameters included in the eq. (11) and (12)

Fiber Diameter [μm]	7
Applied Pressure [MPa]	2, 4
Atmospheric Pressure [MPa]	0.1
Maximum Fiber Volume Fraction [%]	83
Initial Fiber Volume Fraction [%]	45
Fiber Bed Constant [kN/m^2]	13

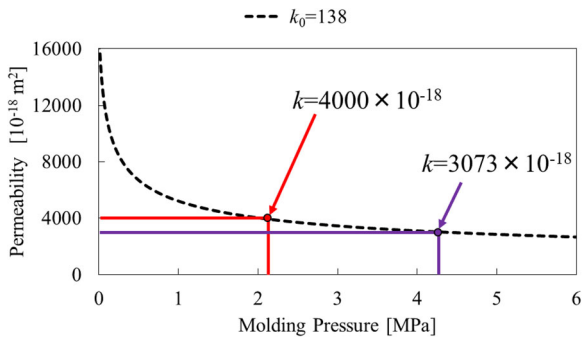

Fig. 7 Permeability for 3 K carbon fiber yarn as a function of molding pressure

in Table 5 (Lin et al. 1994). Figure 8 shows the permeability coefficient as a function of molding pressure. The permeability decreased with increasing pressure, whereas the difference in permeability at the present molding pressure was lower than at the lower pressure condition. As a result, the molding pressure acted as the driving force for resin impregnation more than reducing permeability.

The analytical results for the resin impregnation process were in good agreement with experimental results as shown in Figs. 5 and 6. The M values shown in Table 3 were the same for both molding pressures and molding methods. This result suggests that the capillary effect on resin impregnation is independent of molding pressure and molding method. In general, capillary effect depends on the combination of materials and the size of capillary. In the present molding condition, the size of capillary which corresponds to the distance between fibers remained constant irrespective of molding pressure, because the pressure was large enough. It is also confirmed from the permeability show in Fig. 7, which depended on fiber volume fraction as shown in eq. (11).

In the FS and Powder methods, it was found that the experimental resin impregnation ratio remained almost constant after molding time 120 s at molding pressure

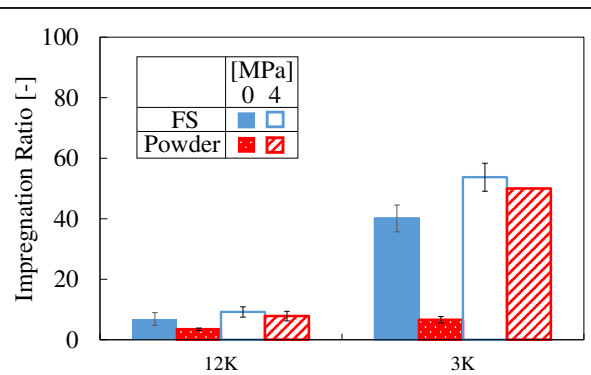

Fig. 8 Effect of number of filament on resin impregnation behavior in 3 K and 12 K composites (Molding time: 0 s)

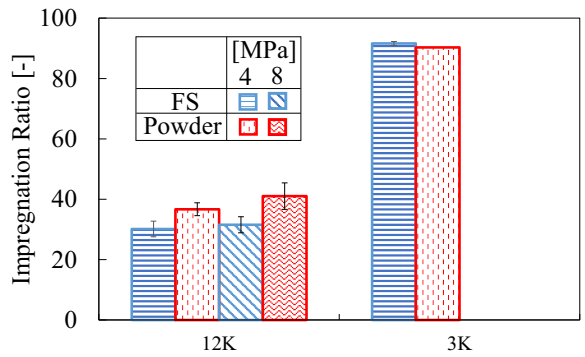

Fig. 9 Effect of number of filament on resin impregnation behavior in 3 K and 12 K composites (Molding time: 300 s)

2 MPa and after 60 s at molding pressure 4 MPa. It was considered that the resin impregnation saturated at that points. As for the MB method, molding time necessary for resin impregnation saturation was longer than for the other molding methods. This is considered to be because the aspect ratio of the MBY is smaller than the carbon fiber yarn for the plain woven fabric used for the other method because braided resin yarns constrained the carbon fiber yarn at the center before weaving. The smaller aspect ratio resulted in the longer resin impregnation distance.

In the present study, the analytical results were in good agreement with the experimental results regardless of molding pressure and methods with same k_0 and M values. This fact means that k_0 and M values are material constant and once the values are determined, resin impregnation behavior for arbitrarily molding condition could be predicted. In other words, we optimize the process parameters for molding of CFRTP with MB, FS and Powder method, once the material paprameters were determined experimentally.

Effect of number of filament (12 K-4 plies–FS, powder)

Figures 8 and 9 show the effect of fiber thickness on impregnation ratio at molding time 0 and 300 s, respectively. Comparing the 12 K and 3 K composites produced with FS method at molding time 0 s and molding

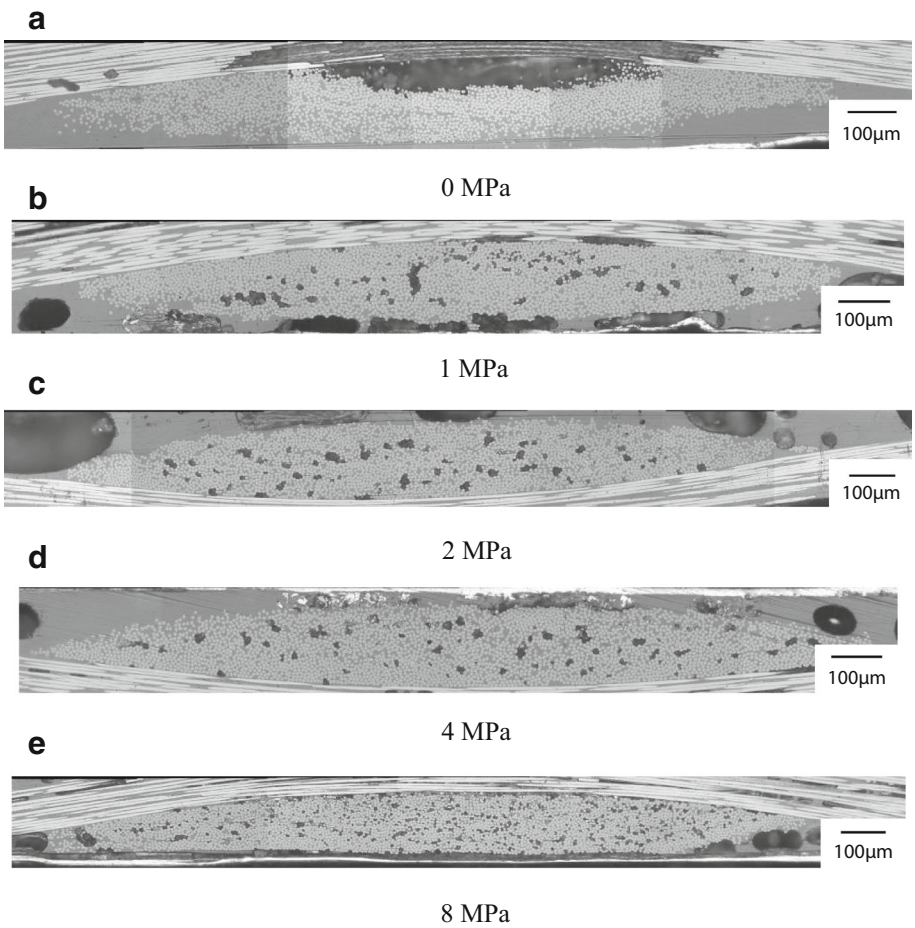

Fig. 10 Cross section of fiber yarn of 3 K composites (FS method-1ply-900 s)

pressure 0 MPa, the resin impregnation ratio for 3 K composites was remarkably higher. Since the 12 K fiber yarns included more air between fibers and longer resin impregnation distance than the 3 K yarns, higher driving force might be required to discharge the air and induce resin flow. In comparison with the Powder specimen under the same condition, the impregnation ratio for 3 K composites with FS method was very high, which result indicated the possibility of higher driving force caused by capillary effect with FS method. Since it is difficult to uniformly dispersed PI resin powder on the entire surface of the carbon fiber fabric, the unevenness of resin powder dispersion might hinder the uniformity of resin flow.

Comparing the resin impregnation ratio under the molding pressure 0 and 4 MPa at molding time 0 s, the resin impregnation ratio for both the 12 K and 3 K composites was improved with increasing molding pressure. However, the improvement in the impregnation ratio for 12 K composites was less than that for 3 K composites. Similarly, comparing the resin impregnation ratio for 12 K composites under molding pressure 4 and 8 MPa at the molding time of 300 s, the improvement with molding pressure was limited. Moreover, comparing the rein impregnation ratio under molding pressure 4 MPa at molding time 300 s, the ratio for the 12 K composites was less than half of that for 3 K composites. These results indicate that higher molding pressure might be necessary for the resin impregnation for 12 K composites.

Effect of molding pressure (3 K-1, 4 plies-FS, powder)

Figures 10 and 11 show the cross section photograph for each molding pressure and resin impregnation ratio measured from cross-sectional observation with FS method. Since the resin impregnation was not improved after the molding pressure 4 MPa, the molding pressure 4 MPa was indicated as the optimum molding pressure. A void in the fiber yarn located at the center of the yarn under molding pressure 0 MPa, whereas fine voids were distributed in the whole of the fiber yarn with increasing molding pressure. This result indicated that the molten resin impregnated to the fiber yarn by the capillary phenomenon at molding pressure 0 MPa and the air between fibers was forced into the center of the yarn. This impregnation behavior began and continued when molding temperature reached the melting point 390 °C for polyimide until reaching the target molding temperature of 410 °C. Thereafter, applying predetermined molding pressure disassemble the void at the center to the fine voids. The fine voids were dispersed to the whole of the yarn and some part of them were pushed out to the yarn, which resulted in the formation of the void in resin rich region.

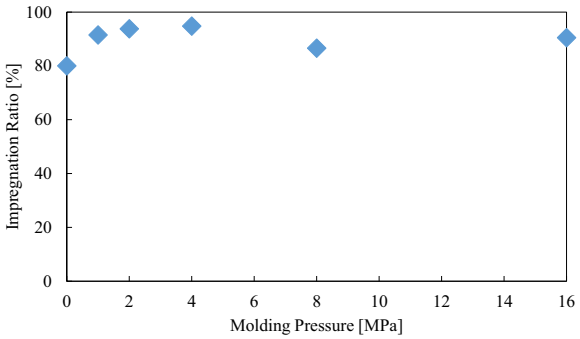

Fig. 11 Effect of molding pressure on resin impregnation behavior in 3 K composites (FS method-1ply-900 s)

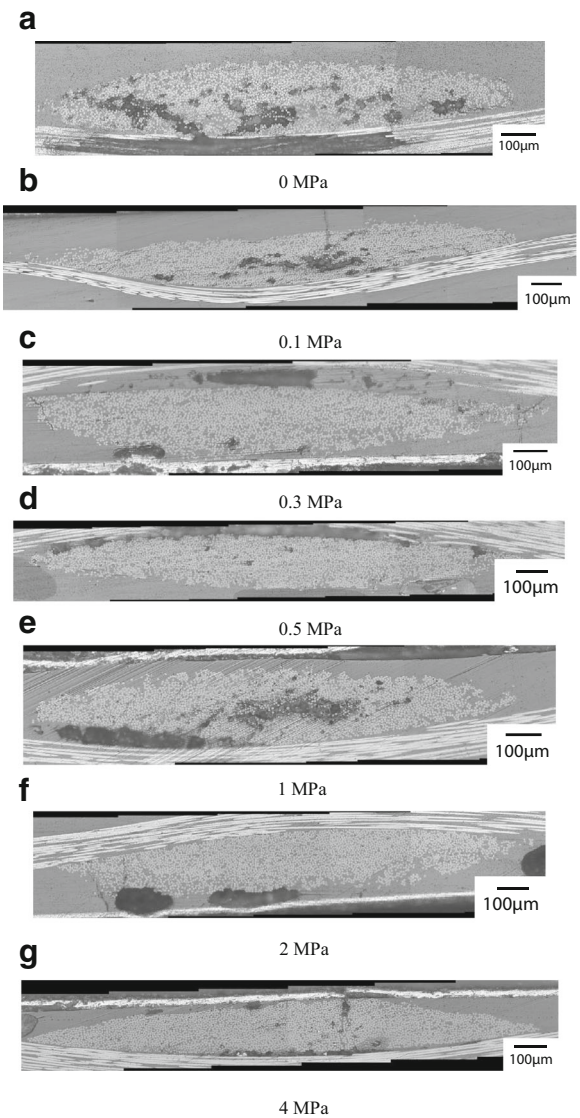

Fig. 12 Cross section of fiber yarn for 3 K composites (Powder method-1 ply-900 s)

Figures 12 and 13 show the cross section photograph for each molding pressure. Figure 14 shows the effect of molding pressure on the resin impregnation behavior with Powder method. Here, molding under much lower molding pressure conditions was conducted. From Fig. 14, it is confirmed that the impregnation ratio reached the maximum at the molding pressure of 0.3 MPa, and the impregnation ratio showed a substantially constant value at the molding pressure more than 0.3 MPa. Therefore, resin impregnation could be sufficiently completed at the molding pressure of 0.3 MPa with the Powder method when sufficient molding time was given. On the other hand, many fine voids were generated in the fiber yarns. This might be due to no pressure loading during cooling. Therefore the effect of pressurizing cooling on void formation is discussed in the following.

Effect of pressurizing cooling (3 K-4 plies-MB, FS, powder)

The influence of pressure loading during cooling on the resin impregnation behavior with MB, FS and Powder method was also discussed. Figure 15 shows the cross-section of the composites with each molding method. These composites were molded with keeping molding pressure during cooling until 255 °C. With all method. Less voids were observed comparing with un-pressurizing cooling. Although slight

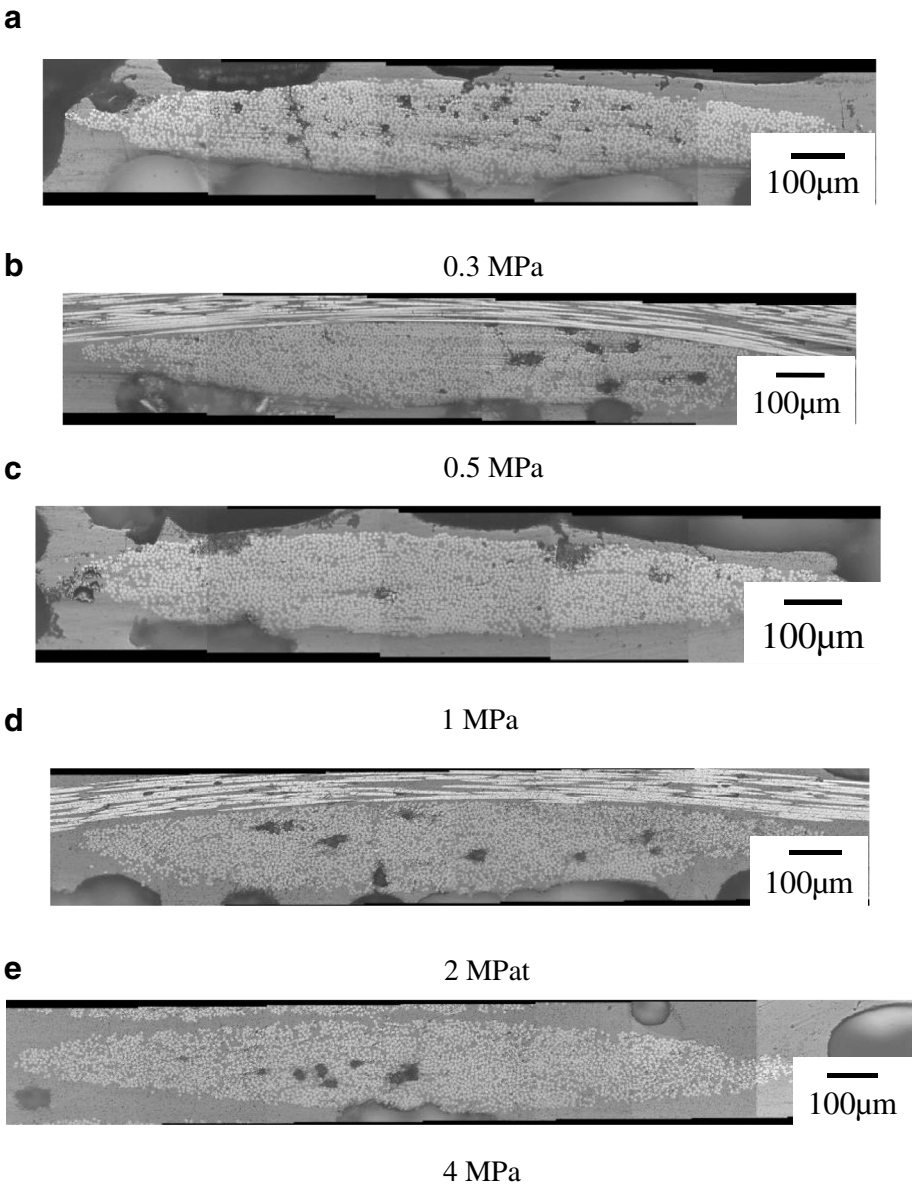

Fig. 13 Cross section of fiber yarn of 3 K composites (Powder method-4 plies-900 s)

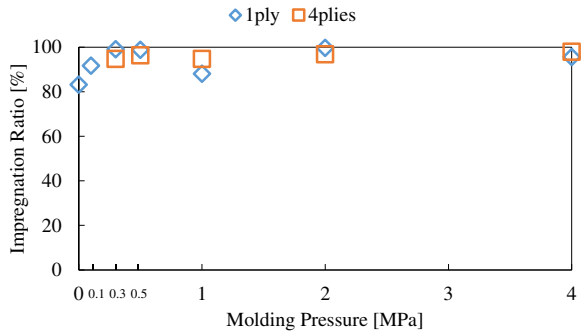

Fig. 14 Effect of pressure on resin impregnation behavior in 3 K composites (Powder method-1, 4 plies-900 s)

un-impregnation region existed at the center of the fiber yarn with MB method, fine voids inside the fiber yarn could be completely eliminated during this pressurizing cooling process.

With Powder and MB method, many cracks induced by thermal residual stress were observed, whereas no cracks existed in the composite with FS method. The difference in crack formation was in the difference in the magnitude of thermal residual stress. Figure 16 shows the results of differential scanning calorimetry measurement on PI resin fiber, film and powder. From Fig. 16, it is clarified that PI fiber used in this study was amorphous phase, whereas PI powder and film were crystalline phase which corresponded to the drop in the heat flow around 400 °C. In Fig. 16, the glass transition temperature which corresponded to the point where the slope of the curve changes were around 259, 248, and 256 °C for PI fiber, film and powder respectively. The glass transition temperature was slightly lower for PI films. Considering the un-pressurizing temperature 255 °C, un-pressurizing just above the glass transition temperature could suppress thermal residual stress and resultant cracks.

Conclusion

In this study, resin impregnation behavior for continuous carbon fiber reinforced polyimide composites was investigated experimentally and analytically. In order to investigate the effect of molding method on the resin impregnation to carbon fiber yarn, specimens were prepared by MB, FS and Powder method. The influence of molding time, pressure, yarn thickness and cooling condition on the resin impregnation process was also discussed. The conclusions obtained were as follows.

1. Molding pressure acted as a driving force for resin flow between fibers rather than for the reduction in permeability.

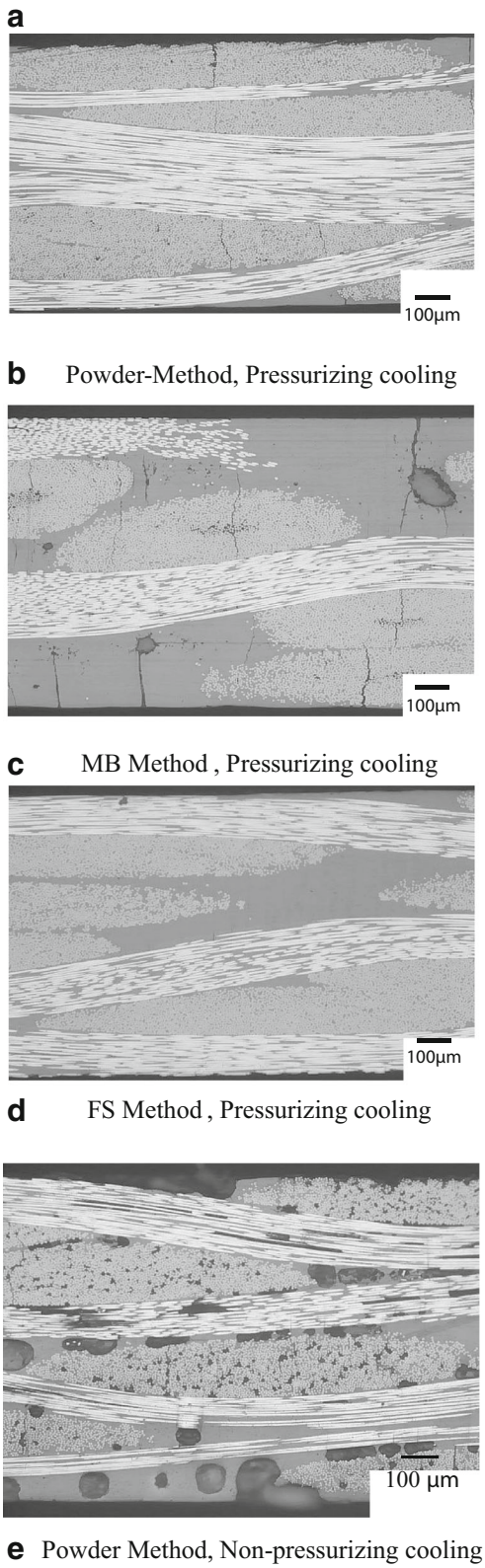

Fig. 15 Cross sections of composites (Pressurizing cooling and Non-pressurizing cooling -2 MPa-300 s)

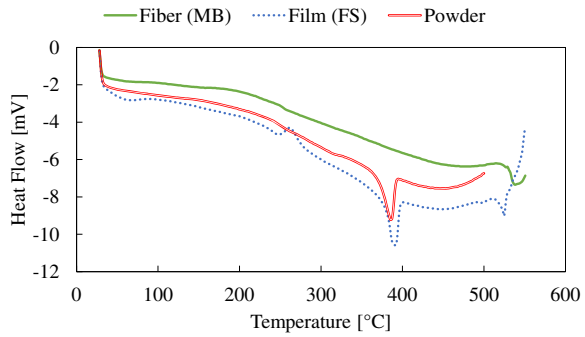

Fig. 16 Heat flow as a function of temperature

2. When the viscocity of the molten resin was known, the resin impregnation behavior to continuous fiber yarn under arbitrary molding conditions could be predicted by the present analytical method, once k_0 and M value were determined in a single set of experiment. The Kozeny constant k_0 was independent of molding pressure and molding method.
3. Higher molding pressure was required for 12 K composites compared with 3 K composites to obtain sufficient resin impregnation.
4. When sufficient molding time conditions were given, sufficient impregnation was obtained for 3 K yarn even at lower molding pressure 0.3 MPa.
5. Fine voids present inside the fiber yarn under the non-pressurizing cooling condition could be completely eliminated by pressurizing cooling process.

Abbreviations
CFRP: Carbon fiber reinforced plastics; CFRTP: Carbon fiber reinforced thermoplastics; CY: Commingled yarn; FS: Film stacking; MB: Micro-braiding; PI: Polyimide

Acknowledgements
Not applicable.

Funding
The work was supported by Tokyo Metropolitan University and Japan Aerospace Exploration Agency.

Availability of data and materials
Please contact author for data requests.

Authors' contributions
SKa carried out the experiments. TO carried out mathematical calculation. SKo conceived the analytical method.KG supervised the work. All authors contributed to the writing and editing of the manuscript. All authors read and approved the final manuscript.

Authors' information
SKa: Graduate student, Tokyo Metropolitan University. TO: Assistant Professor, Tokyo Metropolitan Univeristy. SKo: Professor, Tokyo Metropolitan University. KG: Associate Professor, Japan Aerospace Exploration Agency.

Competing interests
The authors declare that they have no competing interests.

Publisher's Note

Author details
[1]Department of Mechanical Engineering, Graduate School of Science and Engineering, Tokyo Metropolitan University, 1-1 Minami-Osawa, Hachioji, Tokyo 192-0397, Japan. [2]Japan Aerospace Exploration Agency, Sagamihara, Kanagawa, Japan.

Received: 6 April 2018 Accepted: 9 October 2018
Published online: 24 October 2018

References
Åström BT, Buron R, Advani SG (1992) On flow through aligned Fiber beds and its application to composites. J Compos Mater 26(9):1351–1373
Bernet N, Michaud V, Bourban PE, Manson JAE (1999) An impregnation model for the consolidation of thermoplastic composites model from commingled yarns. J Compos Mater 33(8):751–772
Bijewa J, Rattan R (2007) Carbon fabric reinforced polyetherimide composites: optimization of fabric content for best combination of strength and adhesive wsear performance. Wear 262:749–758
Clemans S, Western E, Handermann A (1987) Hybrid yarns for high-performance thermoplastic composites. Mater Sci Monog 41:429–434
Fujihara H, Harada K (2000) Influence of sizing agents on bending property of continuous glass fiber reinforced polypropylene composites. Compos A 31(9):979–990
Fujihara K, Huang ZM, Ramakrishna S, Satknanantham K, Hamada H (2003) Performance study of braided carbon/PEEK composite compression bone plates. Biomat 24:2661–2667
Gebart BR (1992) Permeability of unidirectional reinforcements for RTM. J Compos Mater 26:1100–1133
Gutowski TG (1985) A resin Folw/Fiber deformation model for composites. Mater Sci 16(4):58–64
Gutowski TG, Cai Z, Bauer S, Boucher D, Kingery J, Wineman S (1987) Consolidation experiments for laminate composites. J Compos Mater 21(7): 650–669
Hou M, Ye L, Lee HJ, Mai YW (1998) Manufacture of a carbon-fabric-reinforced polyetherimide (CF PEI) composite material. Compos Sci Technol 58(2):181–190
Hung G (2004) Research on the impregnation behavior of the micro-braided thermoplastic matrix. Mater Design 25:167–170
John DM, Yi Z, Jurron B (1999) Flow of thermoplastics through fiber assemblies. 5th int conference on flow processes in Comppos. Mater:71–78
Kamaya M, Nakai A, Hamada H (2001) Micro-braided yarn as intermediate material System for continuous fiber reinforced thermoplastic composite. 13th Int Conference on Compos Mater:ID –1552
Kim TW, Jun EJ, Um MK, Lee WI (1989) Effect of pressure on the impregnation of thermoplastic resin into a nidirectional fiber bundle. Adv Polym Technol 9(4): 257–279
Kobayashi S, Morimoto T (2014) Experimental and numerical characterization of resin impregnation behavior in textile composite fabricated with micro-braiding technique. Mech Eng J 1(4):14–00071
Kobayashi S, Takada K (2013) Processing of unidirectional hemp fiber reinforced composites with micro-braiding technique. Compos A 46:173–179
Kobayashi S, Takada K, Nakamura R (2014) Processing and characterization of hemp fiber textile composites with micro-braiding technique. Compos A 59:1–8
Kobayashi S, Takada K, Song DY (2012b) Effect of molding condition on the mechanical properties of bamboo-rayon continuous Fiber/poly (lactic acid) composites. Adv Compos Mater 21:79–90
Kobayashi S, Tanaka A (2012) Resin impregnation behavior in processing of unidirectional carbon Fiber reinforced thermoplastic composites. Adv Compos Mater 21:91–102
Kobayashi S, Tanaka A, Morimoto T (2012a) Analytical prediction of resin impregnation behavior during processing of unidirectional fiber reinforced thermoplastic composites considering pressure fluctuation. Adv Compos Mater 21:425–432
Kobayashi S, Tsukada T, Morimoto T (2017) Resin impregnation behavior in carbon fiber reinforced polyamide 6 composite: effects of yarn thickness, fabric lamination and sizing agent. Compos A 101:283–289

Lee JS, Kim JW (2017) Impact response of carbon Fiber fabric/thermoset-thermoplastic combined polymer composites. Adv Compos Letters 26:82–88
Lin Y, Friedrich K (1995) Processing of thermoplastic composites from powder/sheath-fiber bundles. J Compos Mater 48:317–324
Lin Y, Friedrich K, Cutolo D, Savadori A (1994) Manufacture of CF/PEEK composites from powder/sheath fiber preforms. Compos Manuf 5(1):41–50
Lin Y, Friedrich K, Kästel J, Mai YW (1995) Consolidation of unidirectional CF/PEEK composites from commingled yarn prepreg. Compos Sci Technol 54:349–358
Rattan R, Bijwe J (2006) Carbon fabric reinforced polyetherimide composites: influence of weave of fabric and processing parameters on performance properties and erosive wear. Mater Sci Engng A 420:342–350
Sakaguchi M, Nkai A, Hamada H, Takada N (2000) The mechanical properties of unidirectional thermoplastic composites manufactured by a micro-braiding technique. Compos Sci Technol 60:717–722
Svensson N, Shishoo R, Gilchrist M (1998) Manufacturing of thermoplastic composites from commingled yarns –a review. J Thermoplast Compos Mater 11:22–56
Thomas AC, Pavel S, Avdvani SG (2013) Resin film impregnation in fabric prepregs with dual length scale permeability. Compos A 53:118–128
West VBP, Pipes RB, Advani SG (1991) The consolidation of commingled thermoplastic fabrics. Polym Compos 12(6):417–427
Wolfrath J, Michaud V, Modaressi A, JAE M°n (2006) Unsaturated flow in compressible fiber preforms. Compos A 37:881–889